Science in China: *Series D Earth Sciences* 2006 Vol.49 No.7 696—713

DOI: 10.1007/s11430-006-0696-7

Cretaceous volcanic-intrusive magmatism in western Guangdong and its geological significance

GENG Hongyan[1], XU Xisheng[1,2], S. Y. O'Reilly[2], ZHAO Ming[1] & SUN Tao[1]

1.State Key Laboratory of Mineral Deposits Research, Department of Earth Sciences, Nanjing University, Nanjing 210093, China;

2.GEMOC ARC National Key Centre, Department of Earth and Planetary Sciences, Macquarie University, Sydney, NSW 2109, Australia

Correspondence should be addressed to Xu Xisheng (email: xsxu@nju.edu.cn)

Received December 2, 2005; accepted February 23, 2006

Abstract Systematic zircon LA-ICPMS U-Pb dating reveals that Cretaceous volcanic-intrusive activities developed in western Guangdong. Representative volcanic rocks, i.e. Maanshan and Zhougongding rhyodacites, have zircon U-Pb isotopic ages of 100±1 Ma, and the intrusive ones including the Deqing monzonitic granite body and the Xinghua granodiorite body in the Shidong complex, as well as the Tiaocun granodiorite body in the Guangping complex yield ages of 99±2 Ma, ca. 100 Ma, and 104±3 Ma respectively. The biotite-granites of the Shidong complex main body (461±35 Ma) and that of the Guangping complex (444±6 Ma) are Caledonian. In spite of the big time interval between Cretaceous volcanic-intrusive magmatisms and Caledonian intrusive ones, both of them are characterized by enrichment in Rb, Th, Ce, Zr, Hf, Sm, depletion in Ba, Nb, Ta, P, Ti, Eu, and weakly REE tetrad effect. Eu negative anomalies are: Cretaceous volcanic rocks (Eu/Eu^*=0.74), Cretaceous intrusive rocks (Eu/Eu^*=0.35－0.58), Caledonian biotite granites (Eu/Eu^*=0.31－0.34). Studies of Sr-Nd isotope data show that all these igneous rocks have high initial $^{87}Sr/^{86}Sr$ ratios (0.7105－0.7518), and low $\varepsilon_{Nd}(t)$ values (–7.23－–11.39) with their Nd two-stage model ages ranging from 1.6－2.0 Ga, which suggest that they all derived from the Proterozoic crustal basement of southeast China. The occurrence of Cretaceous volcanic-intrusive magmatisms in western Guangdong is related with the important lithospheric extension event in southeast China (including Nanling region) at ca. 100 Ma. The "volcanic line" defined by the large scale Mesozoic intermediate-acidic volcanic magmatisms in southeast China may further extend to the southwest margin of Nanling region.

Keywords: Cretaceous, volcanic-intrusive rocks, zircon U-Pb dating, Sr-Nd isotope, western Guangdong.

The Nanling Mountains lying in the southern part of South China are an economically important granite-related multi-metallogenic province. The Nanling Mountains granites can be described as: temporally spanning from Caledonian to Yanshanian and spatially distributed as three EW trending zones: the north one in Zhuguangshan-Qingzhangshan, the middle one in Dadongshan-Guidong, and the south one in Fogang-

Xinfengjiang with two neighboring zones' midline having an interval of ca. latitude 1°[1]1). The most widely distributed Nanling Mountains granitoids are the early Yanshanian (ca. 160 Ma) granitoids which are thought to be derived from Proterozoic parablastesis[2−4] on the basis of field geology investigation and petrochemical studies. The source of a few small granodiorite bodies (ca. 170 Ma) in the southeast of Hunan Province (belonging to the north belt) may relate to enriched lithospheric mantle induced by subduction fluids, or perhaps to the mixing of asthenospheric magma and middle-lower crust components, or to the partial melting of basaltic rocks contaminated by old crust[5−8]. Alkalic rocks in the Nanling Mountains region (ca. 140Ma) such as A-type granite and syenite in Fogang complex may relate to the upwelling of lithospheric mantle and lithosphere thinning[9−11]. Unlike the case in coastal Southeast China, Late Yanshanian granitoids with limited distribution have not been addressed in detail in the Nanling Mountains.

A series of shoshonitic to high-K calc-alkaline magmatic events (160—125 Ma) developed in the south of western Nanling. The Shilu granodiorite body with its outcrop area of 4.7 km^2 was reported to have the zircon U-Pb age of 125 Ma[12], but Ar^{40}/Ar^{39}plateau age of biotite, potassium feldspar and plagioclase is between 99 Ma and 101 Ma[13]. Li *et al*.[14] regarded 125 Ma as the age of Shilu body, and 100 Ma may reflect some subsequent thermal overprintings. Therefore, it is still necessary to determine whether 100 Ma magmatism exists in western Guangdong, southwestern margin of the Nanling Mountains.

Based on detailed field observation and zircon U-Pb isotope dating, Cretaceous (ca. 100 Ma) volcanic-intrusive magmatism in the southwestern margin of Nanling Mountains is reported in this paper. Its genesis and tectonic setting are discussed in the light of Sr-Nd isotope studies and major and trace elements analyses. These studies may offer some important evidences for a more comprehensive understanding of Mesozoic continental dynamics in South China.

1 General geology

The southwestern margin of the Nanling Mountains crossing the border of Guangdong and Guangxi provinces, belongs to the southwest part of the Yunkai Caledonian fold belt geotectonically, with both volcanic and intrusive rocks developing. The representative Maanshan (17.6 km^2) and Zhougongding (140 km^2) volcanic rocks (Fig. 1) occurring in the Ma'anshan and Jiancheng basin respectively are located in the Lianxian-Yunan volcanic belt. From their field relationships these volcanic rocks were thought to be formed in the early Cretaceous[15], but no isotope datings have been reported. The Shidong and Guangping complexes whose emplacement is controlled by the Lianxian-Yunan fault, intruded into the Jiangkou-Qixing anticline axial core[16] (Fig. 1) with the intruded strata being Cambrian feldspar-quartz sandstone, argillaceous sandstone, and Ordovician quartz sandstone, sandy shale. The Shidong complex was overlain by Devonian sandstone and siltstone[16]. Both complexes extend NE-SW (Fig. 1). Shidong complex has an outcrop area of 2500 km^2 with its largest part being the complex main body (1600 km^2), whose whole rock Rb-Sr age of 443±11 Ma was reported by Wu G. Y. *et al*.[17]. Unfortunately, only two samples were analysed for the isochron, and no other isotopic dating has been given since then. For other bodies of the Shidong complex, viz the Deqing body (398 km^2) in the southwest, the Xinghua body (231 km^2) in the west, and the Wulong body (200 km^2) in the southeast, no isotopic dating work has been carried out (Fig. 1). The Guangping complex has an outcrop area of 851 km^2 with its main body of ca. 845 km^2, and Tiaocun body in the centre of the complex ca. 5 km^2, neither of which has an accurate isotopic dating age.

2 Mineral component and major, trace element geochemistry

2.1 Mineral component

The Maanshan and Zhougongding rhyodacites are grey or grey-green in appearance, with hard, massive structure. Magmatic flow structure is also very distinct. They show porphyritic texture with phenocrysts being potassic feldspar (10%), euhedral plagioclase (15%, An = 40), grained quartz (2%), and flaky biotite (3%) in an aphanitic matrix accounting for 65%, as well as

1) Zhou X M, Sun T, Shen W Z. Petrogenesis of Mesozoic granites-volcanic rocks and the tectonic mechanism transformation in South China. The Proseminar of Development Stratagem on Igneous Rocks Studies——The Third Forum in Granite Petrogenesis and Crust Evolution, Nanjing, 2004

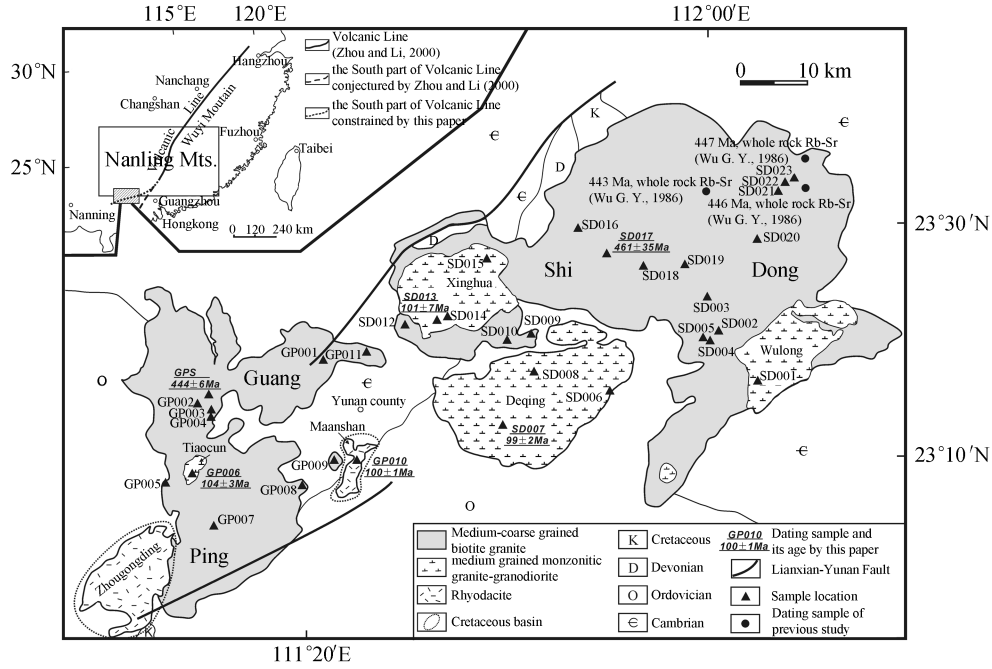

Fig. 1. Geological sketch map of the Shidong, Guangping complexes and adjacent volcanic rocks in western Guangdong (modified after 1:200000 geological maps of Luoding[15], Wuzhou[16], Gaoyao[18], and Huaiji[19] sessions).

rock debris for 5%. Accessory minerals in the rhyodacites are epidote, apatite, magnetite, zircon etc. The Xinghua and Wulong bodies in Shidong complex and the Tiaocun body in Guangping complex are medium grained massive granodiorites with their major mineral components being potassic feldspar (10%—15%), plagioclase (50%—60%, An = 37—44), quartz (20%—25%), biotite (8%), and hornblende (2%—3%) and accessory phases consisting of apatite, magnetite, zircon etc. The Deqing body in Shidong complex is medium grained monzonitic granite with its major mineral components of potassic feldspar (35%—40%), plagioclase (25%—35%, An = 25—30), quartz (25%—30%), biotite (3%—4%); hornblende (~1%), and accessory mineral phases including apatite, magnetite, zircon, etc. The main bodies of Shidong and Guangping complexes are medium-coarse grained biotite granites with their major mineral components being potassic feldspar (40%—45%), plagioclase (15%—20%, An = 25—30), quartz (30%—35%), biotite (3%—4%), and hornblende (1%—2%), and accessory phases apatite, magnetite, sphene, zircon, etc.

2.2 *Major element geochemistry*

Twelve representative fresh samples covering rhyodacite and different intrusive bodies were selected from 74 rock collections for major element geochemistry analysis. The results as well as some previous data are listed in Table 1.

On Middlemost's[23] total alkali-SiO_2 (i.e. TAS) diagram, samples of the Xinghua, Wulong, and Tiaocun bodies fall in the granodiorite field with their SiO_2 ranging from 66.77% to 70.23% and K_2O+Na_2O from 6.22% to 7.28%. Samples of the Deqing body with SiO_2 contents ranging from 70.91% to 73.90% and K_2O+Na_2O from 5.75% to 8.10% fall in the granite field. Samples from the Shidong and Guangping complexes with higher SiO_2 contents of 71.10%—75.40% and K_2O+Na_2O of 7.51%—9.29% plotted in the granite area too. Therefore, the TAS diagram plotting shows identical results to petrographic observations. Besides, all the intrusive rocks (medium grained granodiorite, monzonitic granite, and medium-coarse grained biotite granite) have $K_2O/Na_2O>1$ and are plotted in the sub-alkaline area in the TAS diagram (Fig. 2).

Table 1 Major elements of rhyodacite and Shidong, Guangping complexes (%)[a)]

Sample No.	SiO_2	TiO_2	Al_2O_3	Fe_2O_3	MnO	MgO	CaO	Na_2O	K_2O	P_2O_5	LOI	SUM	ALK	K_2O/Na_2O	A/CNK	Reference
Maanshan rhyodacite																
GP010	67.66	0.46	15.06	3.43	0.12	1.13	1.81	4.16	4.80	0.14	1.25	100.00	8.96	1.15	0.98	this paper
Zhougongding rhyodacite																
29	64.10	0.63	15.89	4.32	0.08	1.92	3.07	3.54	4.16	0.19	1.74	99.81	7.70	1.18	1.00	[20]
30	61.54	0.53	15.29	4.36	0.07	2.01	3.40	2.83	4.16	0.20	5.10	99.62	6.99	1.47	1.00	[20]
31	64.10	0.67	15.89	4.32	0.08	1.68	3.63	3.15	4.13	0.21	1.65	99.68	7.28	1.31	0.98	[20]
32	64.31	0.65	16.07	4.09	0.07	1.94	2.30	3.93	4.30	0.20	2.00	100 01	8.23	1.09	1.05	[20]
33	63.90	0.40	16.18	4.59	0.07	2.13	1.90	3.52	4.62	0.23	2.80	100 47	8.14	1.31	1.14	[20]
Deqing body																
SD006h	70.91	0.52	13.58	4.21	0.11	0.93	2.69	3.34	3.27	0.14	0.80	100.50	6.61	0.98	0.98	this paper
SD007h	73.90	0.20	12.81	2.37	0.11	0.19	1.34	3.08	5.02	0.05	0.65	99.70	8.10	1.63	0.99	this paper
Xinghua body																
SD013h	68.43	0.49	14.40	4.25	0.16	1.50	3.41	3.37	3.39	0.12	1.55	101.10	6.76	1.01	0.93	this paper
SD014h	69.63	0.41	14.04	3.39	0.12	1.21	2.99	2.98	4.26	0.10	0.66	99.80	7.24	1.43	0.94	this paper
SD015	66.77	0.46	14.83	3.79	0.13	1.34	3.38	3.50	3.73	0.12	0.61	98.70	7.23	1.07	0.93	this paper
2972	67.90	0.52	14.73	5.56	—	0.82	3.31	3.37	3.72	—	—	99.93	7.09	1.10	0.94	[16]
Wulong body																
SD001	68.29	0.58	14.43	4.81	0.17	1.47	3.36	3.36	2.86	0.13	0.75	100.20	6.22	0.85	0.98	this paper
Tiaocun body																
GP006	70.23	0.42	14.23	3.44	0.12	1.32	2.83	3.33	3.95	0.10	0.65	100.60	7.28	1.19	0.96	this paper
Shidong complex main body																
SD017h	72.73	0.28	12.09	2.70	0.06	0.39	1.21	2.78	4.79	0.02	2.50	99.60	7.57	1.72	1.01	this paper
SD019	75.40	0.15	12.06	1.74	0.06	0.24	0.65	2.76	4.75	0.01	1.97	99.80	7.51	1.72	1.11	this paper
Null	74.62	0.15	13.18	2.09	0.07	0.50	0.75	3.17	4.90	0.09	—	99.58	8.07	1.55	1.11	[21]
2001	74.26	0.18	12.82	2.52	0.13	0.12	0.83	2.92	5.68	—	—	99.51	8.60	1.95	1.03	[19]
2030	76.28	0.30	12.43	1.87	0.15	0.30	1.43	2.60	4.62	—	—	99.98	7.22	1.78	1.05	[19]
2051	76.84	0.15	12.54	1.46	0.12	0.08	0.34	3.10	5.20	—	—	99.91	8.30	1.68	1.11	[19]
18000	73.68	0.14	13.38	2.02	0.13	0.15	1.19	3.71	4.28	—	1.04	99.81	7.99	1.15	1.04	[19]
4031	71.72	0.20	14.35	2.56	0.19	0.13	1.04	3.43	5.03	—	0.97	99.91	8.46	1.47	1.11	[19]
18134	72.50	0.38	13.65	3.00	0.17	0.38	0.91	2.57	5.23	—	0.83	99.67	7.80	2.04	1.18	[19]
233	73.45	0.20	13.40	2.48	0.04	0.62	1.24	2.46	5.30	0.09	0.69	99.99	7.76	2.15	1.11	[19]
2963	74.76	0.04	12.05	2.38	—	0.09	0.63	3.50	4.64	—	4.48	98.73	8.14	1.33	1.01	[16]
2959	75.52	0.25	12.10	2.94	—	0.14	1.09	3.12	5.05	—	0.26	100.67	8.17	1.62	0.96	[16]
2960	76.14	0.04	12.62	2.68	—	0.18	1.21	2.65	5.10	—	0.14	100.96	7.75	1.92	1.04	[16]
2961	75.32	0.04	12.15	2.70	—	0.18	1.13	3.15	4.98	—	0.21	100.04	8.13	1.58	0.96	[16]
2962	71.90	0.04	14.15	2.82	—	0.12	1.43	3.45	5.04	—	0.39	98.34	8.49	1.46	1.03	[16]
H138	71.05	0.24	14.59	3.61	0.10	0.50	2.00	3.22	4.07	0.03	—	99.41	7.29	1.26	1.09	[22]
4	74.41	0.22	12.69	1.91	0.03	0.27	1.90	2.84	4.25	0.04	—	98.56	7.09	1.50	1.00	[22]
W95-1	74.81	0.10	13.01	1.29	0.04	0.09	1.05	3.14	5.11	0.02	—	98.66	8.25	1.63	1.03	[22]
W46	74.84	0.17	12.60	1.55	0.02	0.18	1.44	3.40	4.79	0.02	—	99.01	8.19	1.41	0.94	[22]
P3-99	75.24	0.10	12.36	1.71	0.03	0.37	0.78	2.81	5.25	0	—	98.65	8.06	1.87	1.05	[22]
W98	75.25	0.13	12.11	1.25	0.02	0.12	0.92	2.21	5.45	0.02	—	97.48	7.66	2.47	1.08	[22]
2	75.75	0.10	12.31	1.10	0.04	0.09	1.34	3.38	4.32	0.02	—	98.45	7.70	1.28	0.97	[22]
P3-101	75.16	0.13	11.54	1.48	0.09	0.28	1.22	3.75	4.57	0	—	98.22	8.32	1.22	0.87	[22]
5	76.19	0.14	12.31	1.50	0.02	0.21	0.90	2.77	5.15	0	—	99.19	7.92	1.86	1.05	[22]
W75a	76.32	0.06	12.54	0.94	0.01	0.03	0.82	3.25	5.18	0	—	99.15	8.43	1.59	1.01	[22]
3	76.67	0.00	12.33	1.82	0.07	0.14	0.38	3.22	4.70	0.05	—	99.38	7.92	1.46	1.11	[22]
D1845	77.23	0.13	11.92	1.12	0.08	0.19	0.37	3.28	5.10	0.02	—	99.44	8.38	1.55	1.03	[22]
Guangping complex main body																
GP002	71.10	0.18	13.82	3.55	0.16	0.08	1.23	4.54	4.75	0.01	1.12	100.50	9.29	1.05	0.93	this paper
GP004h	72.63	0.17	13.69	2.83	0.16	0.39	0.96	3.90	4.43	0.06	1.43	100.70	8.33	1.14	1.06	this paper

a) Analysis was performed at the Modern Analysis Center of Nanjing University via XRF. ALK = Na_2O+K_2O in weight percent, A/CNK = $Al_2O_3/(Na_2O+K_2O+CaO)$ in molecular ratio; "—" implying beyond detection limit.

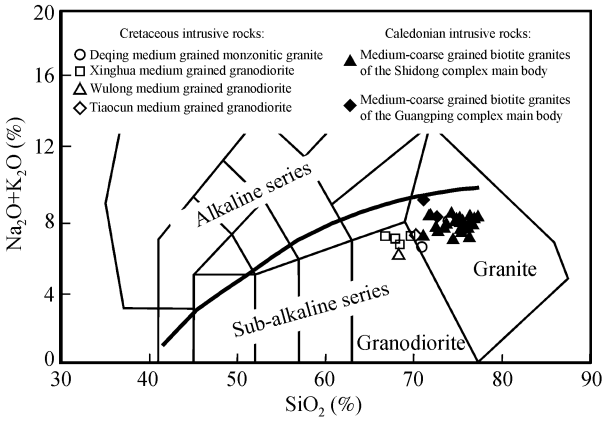

Fig. 2. Total alkali-SiO_2 (TAS) diagram for intrusive rocks. The boundary between alkaline and sub-alkaline series is after Irvine and Baragar[24].

Similarly, the rhyodacite with $K_2O/Na_2O>1$ (Table 1) falls on the boundary of high-K calc-alkaline and shoshonitic series in the SiO_2-K_2O diagram (Fig. 3). Granodiorite-granites fall in the high-K calc-alkaline series too. Cretaceous (see below) intrusive rocks here, i.e. samples of the Deqing, Xinghua, Wulong, and Tiaocun bodies all fall in the high-K calc-alkaline field, which also fall into the range of the Late Mesozoic calc-alkaline to high-K calc-alkaline intermediate-acidic igneous rocks in the coastal area of Zhejiang and Fujian provinces. The medium-coarse grained biotite granites also fall in high-K calc-alkaline field but with higher SiO_2 content (Fig. 3). Cretaceous volcanic rocks fall on the higher part of that area indicating higher K_2O content. The A/CNK values of rhyodacite,

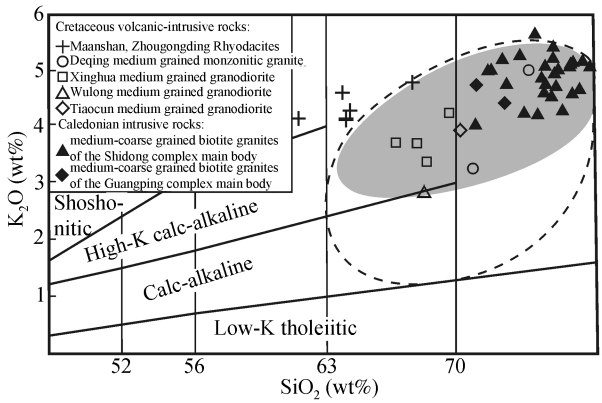

Fig. 3. K_2O-SiO_2 diagram for the Shidong, Guangping complexes and adjacent volcanic rocks in western Guangdong. Classification boundaries are from [25]. Dashed line outlines the field of Late Mesozoic intermediate-acidic igneous rock in the coastal area of Zhejiang and Fujian provinces with 79 data from [26] and [27] included, and thereinto 71 of them fall in the shaded area.

granodiorite, and granites are all less than 1, indicating metaluminous character, while medium-coarse grained biotite granite having the A/CNK values of 1—1.1 is lightly peraluminous (Table 1).

2.3 Trace element geochemistry

The trace element analyses for representative samples, together with previously published data are shown in Table 2. On the N-MORB normalization spider diagram (Fig. 4(a)), Ma'anshan rhyodacite, rich in Rb, Th, Ce, Zr, Hf, Sm and depleted in Ba, Nb, Ta, P, Ti, has total REE (ΣREE) of 293.91 μg/g, and the differentiation between light and heavy REE is obvious (Fig. 5(a)) with the ratio of LREE/HREE=15.75 and $(La/Yb)_N$=20.98. Its Eu anomaly is not remarkable (Eu/Eu^*=0.74, Fig. 5(a)), and the REE tetrad effect is weak ($TE_{1,3}$=0.89)[30,31]. Maanshan rhyodacite has a very similar REE pattern to Late Mesozoic intermediate-acidic volcanic rocks in the coastal area of Zhejiang and Fujian provinces (Fig. 5(a)).

Similarly, the Cretaceous intrusive rocks including granodiorite, medium grained monzonitic granite are rich in Rb, Th, Ce, Zr, Hf, Sm and depleted in Ba, Nb, Ta, P, Ti on the N-MORB normalisation spider diagram (Fig. 4(b)), which is also similar to that of Late Mesozoic intermediate-acidic intrusive rocks in the coastal area of Zhejiang and Fujian provinces. In addition, their REE patterns are quite similar to each other (Fig. 5(b)), with the total REE being 70.77—237.17 μg/g and the average value being 185.19 μg/g which is lower than that of rhyodacite. Their LREE/HREE = 5.73—13.28 (average value of 9.36) and $(La/Yb)_N$ = 5.86—15.17 (average value of 10.07) and therefore the light versus heavy REE differentiation is fairly weak (Fig. 5(b)). The Eu negative anomaly is notable (Eu/Eu^*=0.35—0.58, Fig. 5(b)), but the REE tetrad effects are quite weak ($TE_{1,3}$=0.99—1.02)[30,31].

Likewise, medium-coarse biotite granites of the main bodies of the Shidong and Guangping complexes have similar characteristics of trace element geochemistry with those of rhyodacite and Cretaceous intrusive rocks (Fig. 4(b)), but have less Nb, Ta depletion and more notable depletion of Ba, P. The two main bodies have total REE of 110.52—437.75 μg/g with an average of 274.13 μg/g. Their differentiation of light versus

Table 2 Trace and rare earth elements (μg/g) of rhyodacite and Shidong, Guangping complexes[a)]

Sample No.	Sr	Rb	Ba	Th	Ta	Nb	Zr	Hf	Y	La	Ce	Pr	Nd	Sm	Eu	Gd	Tb	Dy	Ho	Er	Tm	Yb	Lu	∑REE	LREE /HREE	δEu	TE1,3 $(La/Yb)_N$
Ma'anshan rhyodacite																											
GP010	493.71	178.73	1638.18	24.76	1.54	15.90	368.85	8.71	24.74	73.75	132.81	13.09	46.89	8.13	1.69	6.02	0.65	4.26	0.87	2.61	0.38	2.38	0.39	293.91	15.75	0.74	0.89	20.98
Deqing body																											
SD006h	82.50	161.19	624.94	20.47	1.11	11.19	202.37	4.70	36.22	49.39	104.59	10.59	39.25	7.40	1.12	6.98	1.08	6.35	1.37	4.05	0.61	3.84	0.58	237.17	8.55	0.47	0.99	8.70
SD007h	49.80	234.21	659.46	22.76	1.17	10.26	211.23	5.37	41.57	36.37	80.43	8.36	33.35	7.61	0.90	7.97	1.35	8.07	1.61	4.72	0.65	4.20	0.60	196.18	5.73	0.35	1.02	5.86
Xinghua body																											
SD013h	240.39	154.26	440.55	24.09	1.31	12.01	177.46	4.30	19.76	46.02	100.36	9.62	33.57	6.14	0.84	4.83	0.69	3.68	0.75	2.17	0.30	2.05	0.31	211.34	13.28	0.47	1.01	15.17
SD014h	258.07	177.33	863.28	14.26	1.19	11.20	125.41	3.01	19.78	26.11	57.94	6.29	23.98	5.28	0.92	4.61	0.69	3.78	0.77	2.16	0.32	2.13	0.30	135.29	8.16	0.57	1.00	8.27
SD015	263.65	167.25	509.05	22.79	1.21	11.94	169.46	4.03	18.48	31.42	68.55	7.08	25.39	4.89	0.85	4.15	0.63	3.37	0.68	2.02	0.29	2.01	0.30	151.62	10.27	0.57	1.02	10.56
Wulong body																											
SD001	140.59	121.90	473.93	23.22	1.40	11.41	257.65	5.54	26.79	44.29	90.18	8.79	31.07	5.65	1.00	5.27	0.80	4.78	0.95	2.89	0.44	2.93	0.41	199.46	9.80	0.56	1.01	10.22
Tiaocun body																											
GP006	287.03	168.53	488.88	30.81	1.75	15.60	156.11	3.80	21.61	34.29	73.27	7.46	28.13	5.67	1.00	4.86	0.74	4.10	0.80	2.31	0.33	1.98	0.31	165.25	9.71	0.58	1.01	11.69
Shidong complex main body																											
W98*	37.00	268.00	575.00	41.00	4.00	8.00	108.00	15.00	20.20	18.90	64.00	7.10	16.50	5.90	0.37	5.00	2.30	10.30	1.20	3.10	0.74	2.70	0.40	138.51	4.38	0.21	1.92	4.73
W95-1*	37.00	295.00	246.00	46.00	6.00	14.00	108.00	12.00	3.00	20.10	64.00	7.00	17.10	6.20	0.34	5.90	2.00	10.40	1.43	4.46	0.82	2.86	0.66	143.27	4.02	0.17	1.66	4.75
W46*	52.00	194.00	643.00	23.00	6.00	5.00	127.00	12.00	19.10	20.72	56.77	7.11	20.66	6.81	0.33	6.42	1.53	9.41	1.48	3.41	0.74	3.25	0.55	139.19	4.20	0.15	1.35	4.31
W95-2*	–	–	–	–	–	–	–	–	–	17.60	45.20	6.40	13.70	5.40	0.36	5.20	2.20	7.80	1.38	3.81	0.88	3.20	0.60	113.73	3.54	0.21	1.61	3.72
W97*	–	–	–	–	–	–	–	–	–	11.90	40.60	5.80	12.50	5.60	0.19	5.60	2.20	13.20	1.52	4.30	0.86	4.40	0.58	109.25	2.35	0.10	1.89	1.83
Guangping complex main body																											
GP002	69.72	177.13	375.98	29.33	4.16	52.68	435.42	10.62	46.21	103.82	193.21	20.39	72.10	12.77	1.31	10.59	1.58	8.85	1.77	4.96	0.73	4.93	0.74	437.75	11.82	0.34	0.98	14.22
GP004h	125.73	241.46	222.57	28.26	2.93	30.27	130.36	3.40	13.45	25.98	48.24	4.69	17.30	4.06	0.38	3.64	0.51	2.52	0.43	1.20	0.17	1.20	0.19	110.52	10.22	0.31	1.00	14.64

a) Analysis was accomplished in the State Key Laboratory of Mineral Deposits Research, Department of Earth Sciences, Nanjing University, via Finnigan Element Ⅱ ICP-MS, and "—"not analysed. * showing samples from [17].

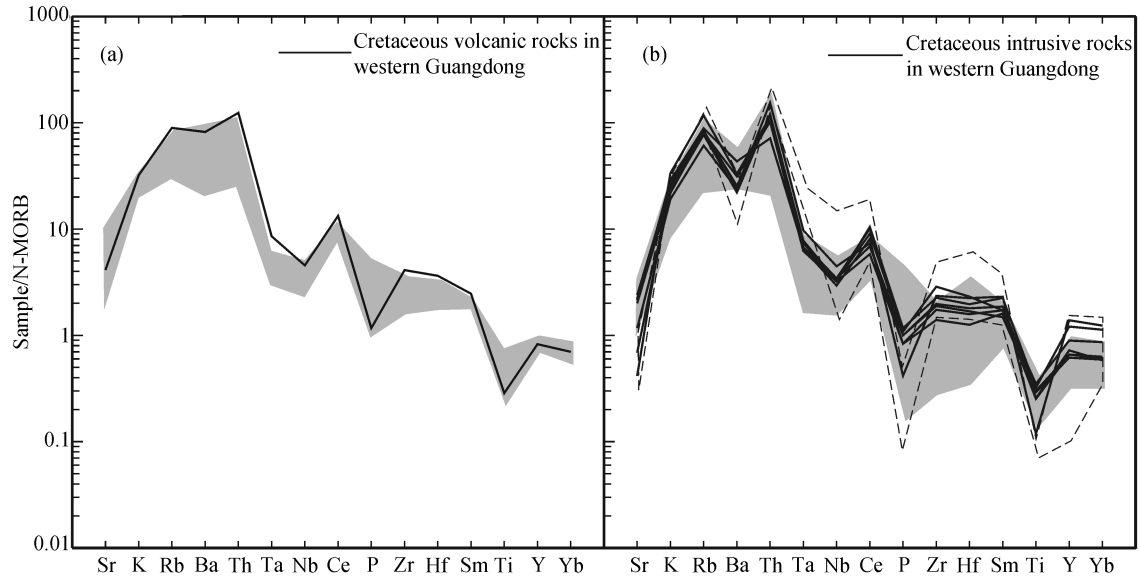

Fig. 4. Spider diagrams of (a) Cretaceous volcanic and (b) Cretaceous and Caledonian intrusive rocks in western Guangdong. N-MORB normalized factors from [28]. Shaded area in (a) and (b) show the spider diagrams of Late Mesozoic intermediate-acidic volcanic and intrusive rocks respectively in the coastal area of Zhejiang and Fujian Provinces. The shaded area in (a) brackets 7 samples from [26] and [27], and that of (b) includes 11 samples from [26]. The dashed line area in (b) exhibits the spider diagram of Caledonian intrusive rocks.

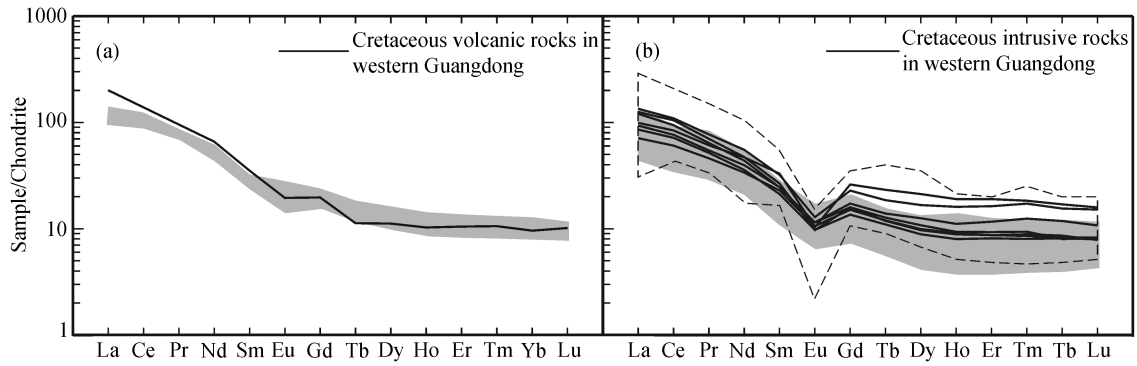

Fig. 5. REE patterns of (a) Cretaceous volcanic and (b) Cretaceous and Caledonian intrusive rocks in western Guangdong. Chondrite normalized factors from [29]. Shaded area in (a) and (b) show the REE patterns of the Late Mesozoic intermediate-acidic volcanic and intrusive rocks respectively in the coastal area of Zhejiang and Fujian Provinces. The shaded area in (a) brackets 7 samples from [26] and [27], and that in (b) includes 11 samples from [26]. The dashed line area in (b) shows the REE pattern of Caledonian intrusive rocks.

heavy REE is not obvious (Fig. 5(b)), LREE/ HREE = 10.22－11.82 with an average of 11.02 and $(La/Yb)_N$ = 14.22－14.64 with the average being 14.43. Their Eu anomalies are quite distinct (Eu/Eu^* = 0.31－0.34, Fig. 5(b)), and REE tetrad effects are quite weak ($TE_{1,3}$=0.98－1.00)[30,31].

3 U-Pb isotope dating

Are the medium grained granodiorite, monzonitic granite, and rhyodacite the products of congenetic magma? What is their relationship to the medium-coarse grained biotite granite? The key to these questions is detailed systematic dating. U-Pb isotope dating for selected representative samples of volcanic and intrusive rocks have, therefore, been carried out. The sampling geographical coordinates are: Ma'anshan rhyodacite 23°09′45.1″N, 111°31′32.8″E; Deqing body 23°12′52.0″N, 111°45′18.9″E; Xinghua body 23°22′－3.1″N, 111°31′30.9″E; Tiaocun body 23°08′23.2″N, 111°16′12.7″E; Shidong complex main body 23°28′－3.8″N, 111°55′11.2″E; Guangping complex main body

23°15′29.8″N, 111°17′32.5″E.

3.1 Zircon selection and analytical techniques

After being panned and magnetically separated, the selected heavy mineral concentrates were further carefully sorted under a Nikon binocular microscope. During this step, a number of representative groups were selected to cover different morphological populations (including variations in elongation, color and crystal face development). These were then mounted in epoxy blocks and polished to the center part of each population for BSE image analysis carried out by using a Camebax SX 100 electron microprobe (EMP) at GEMOC Macquarie University. The U-Pb dating of single zircon is more efficient when combined with BSE/CL images[32]. So we further chose the zircon populations to be dated according to their internal structures, and the representative samples are shown in Fig. 6. The U-Pb dating was performed in the GEMOC Key Centre also, and detailed analysis conditions and procedures are available in [33].

3.2 Analytical results

The U-Pb dating results of representative populations by LA-ICP-MS are listed in Table 3. Concordia plots for rhyodacite and Shidong, Guangping complexes were processed using Ludwig's Isoplot 2.32[34], which shows that most of the zircon populations are on or near concordia indicating that the U-Pb isotope system has not been disturbed, i.e. there has been no addition or loss of U or Pb after their crystallization. Generally, for zircon LA-ICP-MS U-Pb isotope dating, $^{207}Pb/^{206}Pb$ age is more effective for older (>1 Ga) populations, while $^{206}Pb/^{238}U$ age is more precise for younger ones[35]. Therefore, we calculated the $^{206}Pb/^{238}U$ weighted average ages for rhyodacite and the Shidong and Guangping complexes.

Among the 18 analysed zircons for Maanshan rhyodacite, 17 of them are plotted on or near the concordia, with only one (GP010-28) deviating from the curve (Fig. 7, Table 3). Excepting the concordant GP010-22 which probably is a relict zircon with an Indosinian age (240 Ma), the other 16 concordant zircons show a weighted average $^{206}Pb/^{238}U$ age of 100±1 Ma, which agrees with the field evidence: the Ma'anshan rhyodacite overlies an Early Cretaceous (K_1) fossiliferous argillaceous sandstone and conglomerate but is covered by Late Cretaceous (K_2) conglomerate[15]. The Zhougongding rhyodacite has the same field occurrence as the Ma'anshan rhyodacite, and they share similar petrological and geochemical characteristics, which imply that they are co-genetic.

15 zircons have been analysed from the Deqing body. Excepting SD007h-20 and SD007h-26 which deviate from concordia, the other 13 zircons are on or near concordia (Fig. 7, Table 3) with SD007h-30 yielding an age of 109 Ma. The other 12 gave a weighted average of 99±2 Ma.

5 zircons from the Xinghua body were analysed, but only SD013-24 plotted on concordia with an age of 130 Ma. However, field relations and geochemical characters show that the Xinghua body may be co-genetic with the Deqing and Tiaocun (see below) bodies. The zircon of SD013-24 (130 Ma) may be a relict one without obvious isotopic disturbance latterly. The other 4 zircons near concordia (Fig. 7, Table 3) have identical $^{206}Pb/^{238}U$ age (Table 3) with their weighed average age being 101±7 Ma, which is confirmed by the mineral-whole rock Rb-Sr isochron age (see below).

18 zircons from the Tiaocun body were analysed. Two populations, GP006-04 and GP006-18, deviate from concordia (Fig. 7, Table 3), and the latter, round-shaped in appearance (Fig. 7), shows the $^{207}Pb/^{206}Pb$ age of 1030±24 Ma and $^{206}Pb/^{238}U$ age of 515±6 Ma, indicating it is a relict zircon with the minimum age of Early Paleozoic. GP006-12 has a concordant age of 128 Ma and may also be a relict zircon with no obvious isotopic disturbance. The other 15 zircons yield $^{206}Pb/^{238}U$ ages ranging from 96 Ma to 114 Ma with the weighted average age of 104±3 Ma.

5 zircons have been analysed for the Shidong complex main body, only SD017-16 showing an obvious deviation from concordia. The other 4 zircons plot on or near concordia (Fig. 7, Table 3). SD017h-14 yields an age of 537 Ma. The other 3 concordant zircons show the weighted average age of 461±35 Ma, which is consistent with the field relationships, i.e., the western part of the Shidong complex main body intruded into Cambrian feldspar-quartz sandstone, and is covered by Devonian sandstone[16]. The zircon U-Pb dat-

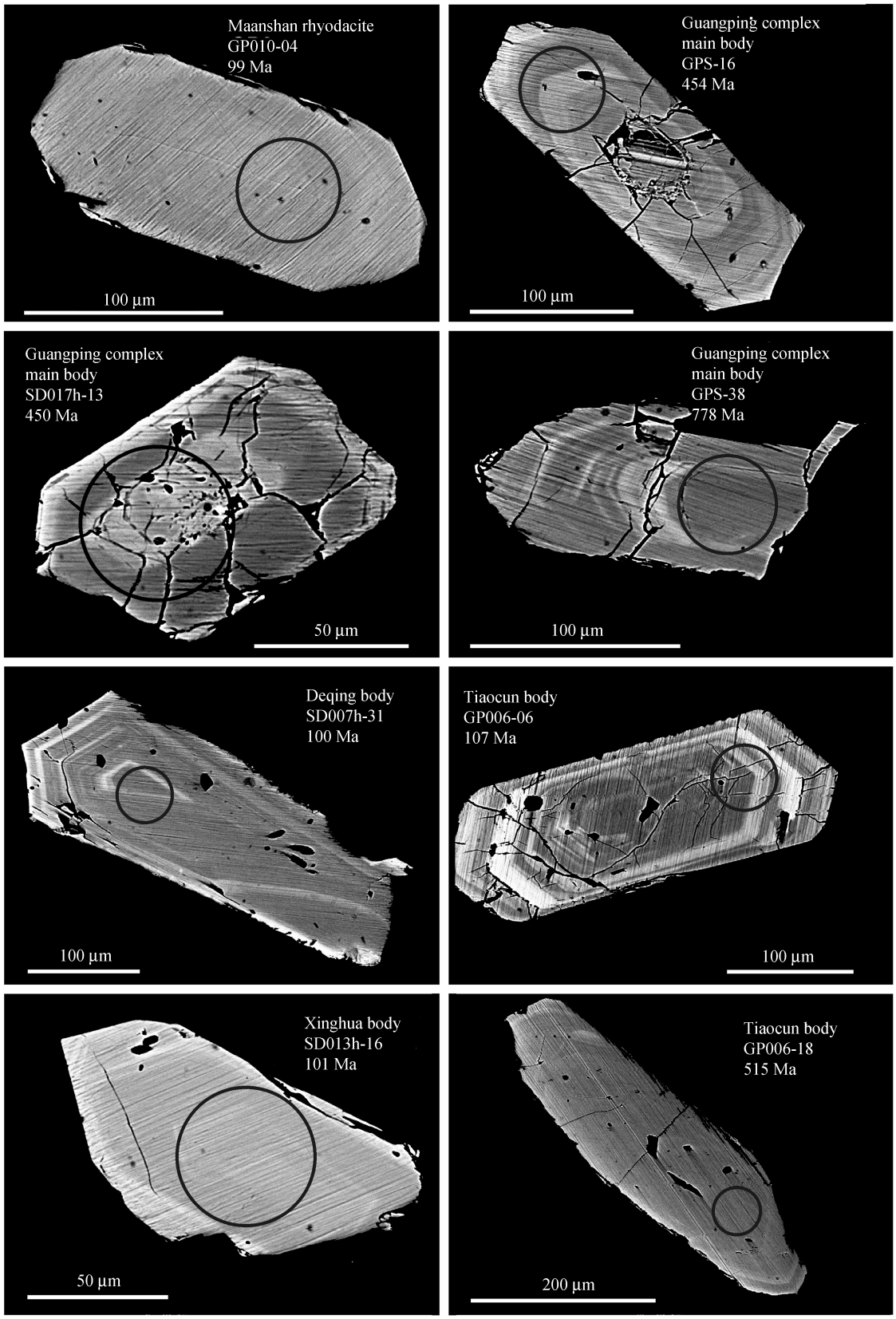

Fig. 6. BSE images of representative populations for rhyodacite and Shidong, Guangping complexes.

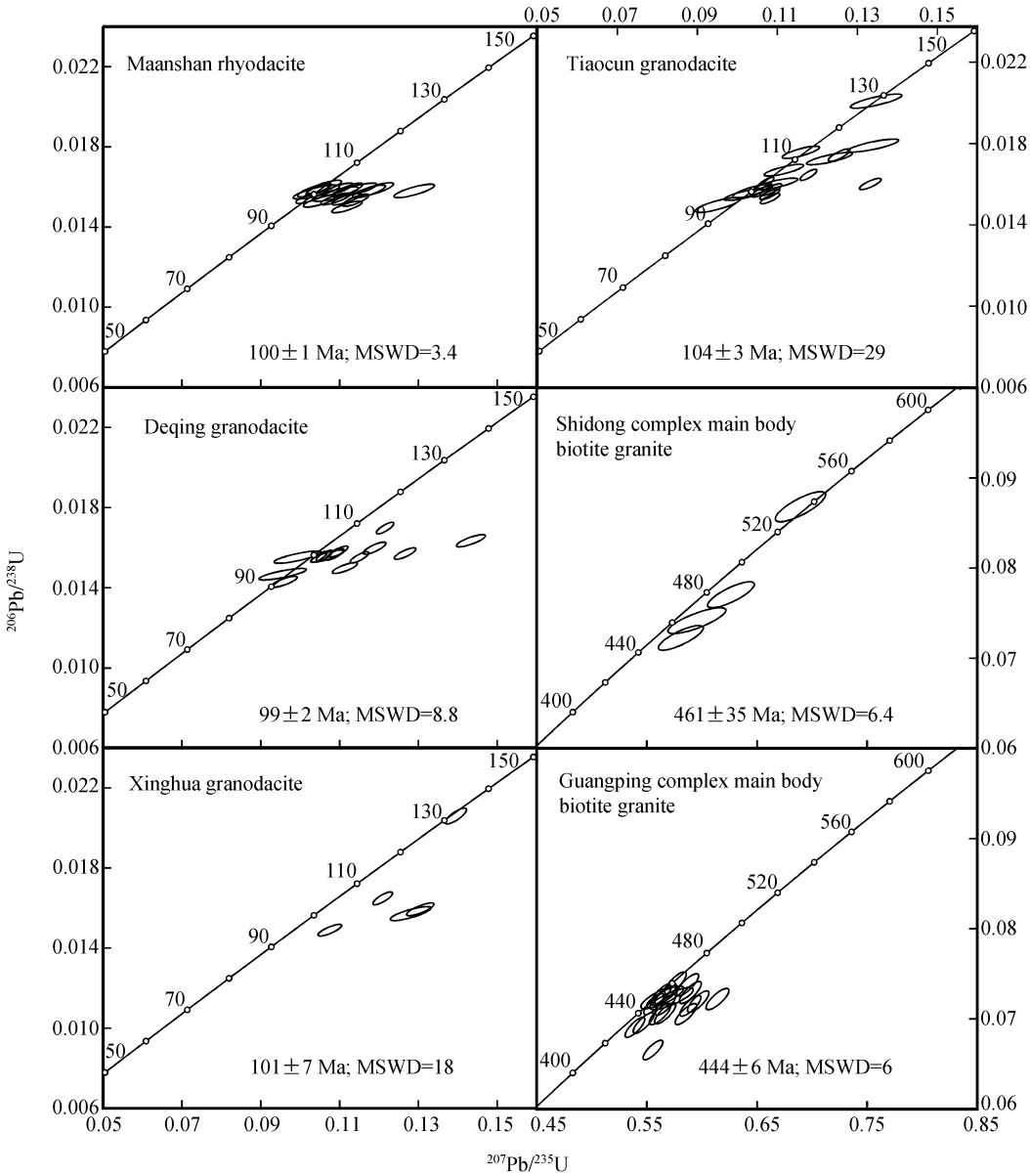

Fig. 7. Concordia diagrams for zircon age populations of rhyodacite and Shidong, Guangping complexes.

ing result is also consistent with the previous whole rock Rb-Sr isochron age (443±11 Ma)[17]. Therefore, the Shidong complex main body was the product of Caledonian magmatism. From the Guangping complex main body, 20 zircons have been analysed. All of them are plotted on the concordia (Fig. 7, Table 3). 19 of them have $^{206}Pb/^{238}U$ ages ranging from 415 Ma to 460 Ma with a weighted average age of 444±6 Ma. GPS-38 has Late Proterozoic (778 Ma) age.

Summarizing the above, zircon LA-ICP-MS U-Pb dating shows that the age of the Ma'anshan and Zhougongding rhyodacites is 100±1 Ma, and those of the Deqing and Tiaocun bodies are 99±2 Ma, 104±3 Ma respectively. The Xinghua body most probably formed at about 100 Ma as well. All of them are the products of Cretaceous magmatisms. The main bodies of the Shidong and Guangping complexes with the age of 461±35 Ma and 444±6 Ma, are the products of Caledonian magmatisms. Therefore, two magmatism episodes exist in western Guangdong, but they cannot be related through differentiation because of the big intervening time interval even if they are spatially close.

Table 3 U-Th-Pb isotope data for zircons of rhyodacite and Shidong, Guangping complexes[a)]

	U-Th-Pb ratio				Age (Ma)			
	$^{207}Pb/^{206}Pb\pm1\sigma$	$^{207}Pb/^{235}U\pm1\sigma$	$^{206}Pb/^{238}U\pm1\sigma$	$^{208}Pb/^{232}Th\pm1\sigma$	$^{207}Pb/^{206}Pb\pm1\sigma$	$^{207}Pb/^{235}U\pm1\sigma$	$^{206}Pb/^{238}U\pm1\sigma$	$^{208}Pb/^{232}Th\pm1\sigma$
Ma'anshan rhyodacite								
GP010-03	0.05411±122	0.11185±254	0.01500±19	0.00504±7	376±52	108±2	96±1	102±1
GP010-04	0.04817±118	0.10276±254	0.01548±20	0.00493±9	108±59	99±2	99±1	99±2
GP010-06	0.05450±132	0.11928±290	0.01588±22	0.00515±9	392±56	114±3	102±1	104±2
GP010-08	0.05266±118	0.11175±248	0.01540±19	0.00498±8	314±52	108±2	99±1	100±2
GP010-13	0.05129±116	0.10892±246	0.01540±19	0.00497±7	254±53	105±2	99±1	100±1
GP010-14	0.04990±140	0.10523±293	0.01530±20	0.00509±9	190±67	102±3	98±1	103±2
GP010-16	0.05005±111	0.10962±245	0.01589±20	0.00506±9	197±53	106±2	102±1	102±2
GP010-22	0.05076±98	0.26520±522	0.03789±47	0.01231±21	230±46	239±4	240±3	247±4
GP010-23	0.04783±94	0.10468±211	0.01587±20	0.00522±8	91±48	101±2	102±1	105±2
GP010-25	0.04809±132	0.10608±290	0.01600±22	0.00505±10	104±65	102±3	102±1	102±2
GP010-26	0.04792±181	0.10410±388	0.01575±23	0.00498±12	95±85	101±4	101±1	100±2
GP010-28	0.05921±158	0.12895±338	0.01580±22	0.00571±12	575±59	123±3	101±1	115±2
GP010-33	0.04738±121	0.10337±264	0.01582±21	0.00502±9	68±59	100±2	101±1	101±2
GP010-35	0.05206±177	0.11371±382	0.01584±23	0.00546±13	288±80	109±3	101±1	110±3
GP010-36	0.05398±126	0.11746±275	0.01578±21	0.00562±9	370±54	113±2	101±1	113±2
GP010-39	0.05051±183	0.10892±387	0.01564±24	0.00532±13	219±86	105±4	100±2	107±3
GP010-40	0.05395±101	0.11410±220	0.01534±20	0.00557±8	369±43	110±2	98±1	112±2
GP010-41	0.05132±105	0.11232±234	0.01587±21	0.00561±9	255±48	108±2	102±1	113±2
Deqing medium grained monzonitic granite								
SD007h-06	0.04977±128	0.10695±273	0.01559±20	0.00501±13	184±61	103±3	100±1	101±3
SD007h-07	0.05374±70	0.11506±155	0.01552±18	0.00546±6	360±30	111±1	99±1	110±1
SD007h-11	0.05385±102	0.11135±212	0.01499±18	0.00504±7	365±44	107±2	96±1	102±1
SD007h-12	0.04887±60	0.10476±136	0.01554±18	0.00504±6	142±29	101±1	99±1	102±1
SD007h-14	0.05030±71	0.10968±160	0.01581±18	0.00514±8	209±33	106±1	101±1	104±2
SD007h-20	0.06356±106	0.14334±241	0.01635±20	0.00645±10	727±36	136±2	105±1	130±2
SD007h-26	0.09875±138	0.22333±321	0.01640±20	0.00704±9	1601±27	205±3	105±1	142±2
SD007h-30	0.05193±57	0.12154±146	0.01698±19	0.00541±6	282±26	116±1	109±1	109±1
SD007h-31	0.04935±60	0.10615±139	0.01560±18	0.00470±6	164±29	102±1	100±1	95±1
SD007h-36	0.05039±65	0.10882±151	0.01567±19	0.00484±6	213±31	105±1	100±1	98±1
SD007h-39	0.05399±81	0.11889±189	0.01598±20	0.00502±7	371±35	114±2	102±1	101±1
SD007h-44	0.04721±205	0.09556±396	0.01468±19	0.00467±6	60±95	93±4	94±1	94±1
SD007h-45	0.04870±112	0.09594±219	0.01430±18	0.00453±7	133±55	93±2	92±1	91±1
SD007h-48	0.0464±193	0.09931±393	0.01553±20	0.00495±6	18±89	96±4	99±1	100±1
SD007h-54	0.05845±79	0.12663±182	0.01571±19	0.00579±8	547±30	121±2	100±1	117±2
Xinghua medium grained granodiorite								
SD013-09	0.05250±93	0.10752±198	0.01489±19	0.00449±6	307±41	104±2	95±1	91±1
SD013-16	0.05910±160	0.12802±342	0.01572±23	0.00536±9	571±60	122±3	101±1	108±2
SD013-18	0.05940±97	0.13048±228	0.01593±21	0.00553±8	582±36	125±2	102±1	111±2
SD013-24	0.04915±52	0.13951±178	0.02059± 26	0.00558±7	155±25	133±2	131±2	112±1
SD013-25	0.05324±64	0.12094±165	0.01648±21	0.00579±7	339±28	116±1	105±1	117±1
Tiaocun medium grained granodiorite								
GP006-04	0.06034±80	0.13324±178	0.01601±18	0.00609±8	616±29	127±2	102±1	123±2
GP006-05	0.05428±183	0.13396±421	0.01790±021	0.00559±6	383±77	128±4	114±1	113±1
GP006-06	0.04850±152	0.11163±325	0.01669± 19	0.00529±5	124±74	107±3	107±1	107±1
GP006-07	0.04782±139	0.11586±308	0.01757±20	0.00558±6	90±67	111±3	112±1	112±1
GP006-08	0.05130±75	0.10820±159	0.01530±17	0.00512±6	254±34	104±1	98±1	103±1
GP006-09	0.05188±58	0.11779±138	0.01646±18	0.00525±6	280±26	113±1	105±1	106±1
GP006-10	0.04766±168	0.10179±335	0.01549±19	0.00492±6	82±79	98±3	99±1	99±1
GP006-11	0.05218±72	0.12546±177	0.01743± 20	0.00552±7	293±32	120±2	111±1	111±1
GP006-12	0.04863±163	0.13471±424	0.02009±23	0.00636±9	130±79	128±4	128±1	128±2
GP006-13	0.05170±170	0.12303±378	0.01726±20	0.00543±6	272±77	118±3	110±1	109±1

(*To be continued on the next page*)

(*Continued*)

	U-Th-Pb ratio				Age (Ma)			
	$^{207}Pb/^{206}Pb\pm1\sigma$	$^{207}Pb/^{235}U\pm1\sigma$	$^{206}Pb/^{238}U\pm1\sigma$	$^{208}Pb/^{232}Th\pm1\sigma$	$^{207}Pb/^{206}Pb\pm1\sigma$	$^{207}Pb/^{235}U\pm1\sigma$	$^{206}Pb/^{238}U\pm1\sigma$	$^{208}Pb/^{232}Th\pm1\sigma$
GP006-15	0.05054±76	0.10810±164	0.01551±17	0.00497±7	220±36	104±2	99±1	100±1
GP006-16	0.04967±173	0.10966±359	0.01601±19	0.00506±6	180±83	106±3	102±1	102±1
GP006-17	0.04807±157	0.10386±328	0.01567±22	0.00493±11	103±76	100±3	100±1	99±2
GP006-18	0.07358±85	0.84450±1022	0.08325± 93	0.03300±37	1030±24	622±6	515±6	656±7
GP006-20	0.04605±195	0.09511±373	0.01498±24	0.00488±11	0±90	92±3	96±2	98±2
GP006-21	0.04916±75	0.10603±164	0.01564±18	0.00520±8	155±37	102±2	100±1	105±2
GP006-22	0.04836±59	0.10711±136	0.01607±18	0.00521±6	117±29	103±1	103±1	105±1
GP006-23	0.05000±81	0.10842±178	0.01573±19	0.00513±8	195±39	105±2	101±1	103±2
Shidong complex main body medium-coarse grained biotite granites								
SD017h-09	0.05823±185	0.59548±1735	0.07417±95	0.02299±32	538±71	474±11	461±6	459±6
SD017h-13	0.05830±153	0.58085±1344	0.07226±90	0.02239±28	541±59	465±9	450±5	448±5
SD017h-14	0.05760±146	0.68952±1509	0.08681±110	0.02694±34	515±57	533±9	537±7	537±7
SD017h-16	0.14364±144	1.67436±1955	0.08461±101	0.08614±99	2272±18	999±7	524±6	1670±18
SD017h-19	0.05897±150	0.62639±1399	0.07704±95	0.02384±32	566±57	494±9	478±6	476±6
Guangping complex main body medium-coarse grained biotite granites								
GPS-01	0.05746±58	0.56685±608	0.07158±77	0.02370±25	509±23	456±4	446±5	473±5
GPS-02	0.06056±61	0.55561±590	0.06656±71	0.01946±21	624±22	449±4	415±4	390±4
GPS-03	0.06022±62	0.58551±641	0.07054±77	0.01832±19	611±23	468±4	439±5	367±4
GPS-05	0.05618±58	0.56329±622	0.07273±79	0.02234±25	459±23	454±4	453±5	447±5
GPS-06	0.05633±58	0.55641±606	0.07165±77	0.02184±25	465±23	449±4	446±5	437±5
GPS-07	0.05985±62	0.58962±634	0.07147±76	0.02141±23	598±23	471±4	445±5	428±5
GPS-09	0.05820±62	0.56674±633	0.07063±77	0.02028±22	537±24	456±4	440±5	406±4
GPS-10	0.05663±60	0.53926±587	0.06907±73	0.02049±22	477±24	438±4	431±4	410±4
GPS-12	0.05746±145	0.57246±1304	0.07226± 80	0.02243±23	509±57	460±8	450±5	448±5
GPS-16	0.05863±61	0.58954±660	0.07294±80	0.02228±25	553±23	471±4	454±5	445±5
GPS-17	0.06169±65	0.61418±685	0.07221±78	0.02234±25	663±23	486±4	449±5	447±5
GPS-19	0.05779±63	0.56215±649	0.07055±78	0.02270±26	522±24	453±4	439±5	454±5
GPS-27	0.05624±125	0.56103±1080	0.07235±81	0.02251±25	462±51	452±7	450±5	450±5
GPS-30	0.05647±61	0.57607±652	0.07401±80	0.02384±27	471±24	462±4	460±5	476±5
GPS-31	0.05653±60	0.56702±638	0.07275±79	0.02382±28	473±24	456±4	453±5	476±6
GPS-32	0.05771±60	0.58705±656	0.07379±81	0.02347±27	519±23	469±4	459±5	469±5
GPS-33	0.05672±126	0.56675±1101	0.07247±79	0.02253±24	481±50	456±7	451±5	450±5
GPS-37	0.06016±60	0.59674±644	0.07194±78	0.02170±23	609±22	475±4	448±5	434±5
GPS-38	0.06656±171	1.17736±2655	0.12829±158	0.03915±47	824±55	790±12	778±9	776±9
GPS-44	0.05705±61	0.54704±615	0.06955±75	0.02114±25	493±24	443±4	433±5	423±5

a) Analysis was performed at GEMOC center, Macquarie University, Australia.

4 Sr-Nd isotopes and origin of the magma

Some of the U-Pb isotopic dating samples were selected for further Sr-Nd isotope analysis at the Institute of Geology and Geophysics, Chinese Academy of Sciences, and the analysed results are listed in Table 4. Considering that the zircon U-Pb isotopic dating for the Xinghua body was not robust, we performed biotite-plagioclase-whole rock Rb-Sr isochron dating which yielded an age of 98±7 Ma (Fig. 8). It is consistent with the zircon U-Pb dating result (101±7 Ma) within the errors, and further confirms that the Xinghua body was formed at the age of ca. 100 Ma.

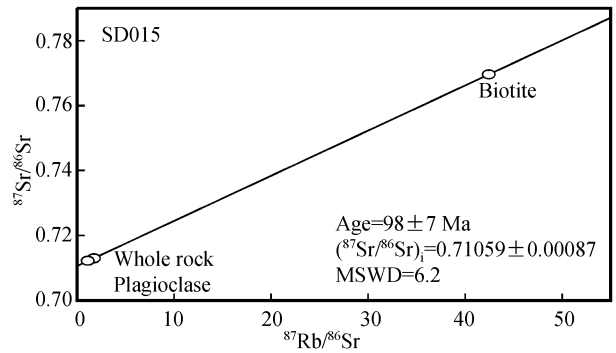

Fig. 8. Rb-Sr isochron by biotite-plagioclase-whole rock of the Xinghua body.

High values (0.7105－0.7518) of initial $^{87}Sr/^{86}Sr$ and low values (–7.23－11.39) of $\varepsilon_{Nd}(t)$ (Table 4) imply that the Cretaceous rhyodacite and granitoids, as well as the Caledonian biotite-granite were all derived from partial melting of crustal materials. Furthermore, all samples' falling in "Proterozoic crust evolution area of South China" (Fig. 9) indicates that they were derived from the partial melting of Proterozoic basement in South China.

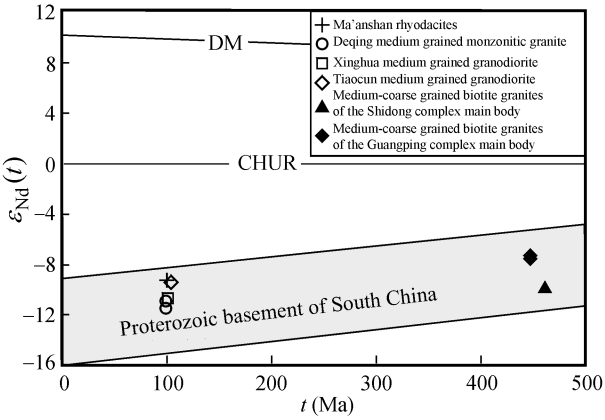

Fig. 9. $\varepsilon_{Nd}(t)$-t diagram for rhyodacite and intrusive rocks. The area of "Proterozoic basement of South China" from Shen W. Z.[36].

The relatively homogeneous Sm/Nd ratios (ranging from 0.16 to 0.24) of the Cretaceous rhyodacite, granitoids, and Caledonian biotite granite indicate that no obvious Nd isotope differentiation has taken place. Their $^{147}Sm/^{144}Nd$ ratios varying from 0.0970 to 0.1441 are within the range of mean upper continental crust (0.118±0.034), and then it would be meaningful to calculate the Nd isotope model age (T_{DM})[37,38]. Alternatively, two-stage Nd isotope model ages (T_{2DM}) may be calculated to further understand the origin of the igneous rocks (Table 4). The calculations show that all the T_{DM} and T_{2DM} varied between 1639 Ma and 2010 Ma except for GP010 (slightly low T_{DM}) and SD007h (slightly high T_{DM}), which again imply that they were derived from the Proterozoic crust basement. The rounded relict zircons of GP006-18 ($^{207}Pb/^{206}Pb$ age of 1030±24 Ma) in the Tiaocun body, GPS-38 (778 Ma) in the Guangping main body, GP010-22 (240 Ma) in the Ma'anshan rhyodacite, and the occurrence of ca. 130 Ma relict zircons in the Xinghua and Tiaocun bodies imply that the Proterzoic basement underwent a series of tectonic thermal overprintings. This conclusion is identical with that reached from studies of Nd isotope model ages, zircon U-Pb and Hf isotopes of multiple-stage granites in the Nanling Mountains[38,39].

5 Tectonic settings of Cretaceous volcanic-intrusive magmatism in western Guangdong

Magmatism in SE China was dormant between 205 and 180 Ma[40−43]. From the Middle Jurassic (ca. 180 Ma), South China was in an extensional tectonic setting, dominated by subduction of the Paleo-Pacific plate[40,44]. Some small-scale magmatism during the early period of the Middle Jurassic (180－170 Ma) was reactivated and became more and more intensive, forming the Late Mesozoic large-scale and long-term magmatism in South China[7,44,45]. During the Middle-Late Jurassic, the Paleo-Pacific plate subducted at low-angle and high speed; subsequently the subduction angle increased. Until the Cretaceous (ca. 100 Ma), magmatism totally migrated oceanward because of the high subduction angle[46,47], that is, Jurassic granitoids mainly spread in the west of Wuyi mountain while Cretaceous volcanic-intrusive rocks developed in the coastal area of Zhejiang and Fujian provinces[48]. These Cretaceous coastal volcanic-intrusive magmatic episodes, which comprise the climax of large-scale magmatisms in SE China, were constrained by the Pacific dynamic system forming under an extensional tectonic setting, and contain abundant information of crust-mantle interaction[49] . The representative intrusive bodies include Fuzhou (104 Ma)[50], Danyang (103 Ma)[50], Gunong bodies (101 Ma)[51] in Fujian Province; Liangnong (101 Ma)[52], Daao bodies (100 Ma)[53] in Zhejiang Province, and bimodal volcanic rocks (103 Ma)[49] in Fujian Province.

Despite being far from the subduction zone, western Guangdong also was dominated by the interaction of Paleo-Pacific and European-Asian plate. What, then, is the tectonic setting of Cretaceous (100 Ma) volcanic-intrusive magmatism in western Guangdong? In general, the whole South China was under extension[40,43]. Geochemistry and tectonic setting studies for the shoshonitic intrusive rocks in southeastern Guangxi and Yangchun basin in western Guangdong show that an extensional tectonic setting had existed

Table 4 Sr-Nd isotopic compositions of rhyodacite and Shidong, Guangping complexes[a)]

Sample No.	Age (Ma)	Rb (μg/g)	Sr (μg/g)	$^{87}Rb/^{86}Sr$	$^{87}Sr/^{86}Sr$	2σ	$(^{87}Sr/^{86}Sr)_i$	Sm (μg/g)	Nd (μg/g)	Sm/Nd	$^{147}Sm/^{144}Nd$	$^{143}Nd/^{144}Nd$	2σ	$\varepsilon_{Nd}(t)$	T_{DM} (Ma)	T_{2DM} (Ma)
Ma'anshan rhyodacite																
GP010	100	168.84	519.56	0.936862	0.712646	10	0.7113	8.16	50.92	0.16	0.096998	0.512102	10	–9.18	1367	1643
Deqing body																
SD007h	99	236.11	51.59	13.274693	0.770459	11	0.7518	8.25	34.67	0.24	0.144142	0.512020	11	–11.39	2464	1822
DQ-1**	99	217.30	65.40	9.671000	0.756568	15	0.7430	6.23	29.06	0.21	0.129800	0.512040	18	–10.82	2010	1775
Xinghua body																
SD015whole rock	98	161.92	269.24	1.746835	0.712948	11	0.7105	5.05	25.66	0.20	0.119185	0.512047	11	–10.57	1775	1754
SD015 biotite		501.69	34.30	42.445645	0.769575	15		—	—	—	—	—	—	—	—	—
SD015 plagioclase		81.54	212.14	1.108614	0.712192	11		—	—	—	—	—	—	—	—	—
Tiaocun body																
GP006	104	—	—	—	—	—	—	6.09	31.61	0.19	0.116674	0.512105	13	–9.35	1639	1660
Shidong complex main body																
SD017h	461	—	—	—	—	—	—	11.57	58.47	0.20	0.119815	0.511909	11	–9.69	2007	1978
Guangping complex main body																
GP-1	447	161.10	70.33	6.672000	0.753642	28	0.7112	3.52	17.37	0.20	0.122500	0.512038	13	–7.48	1853	1787
GP-2	447	132.90	65.45	5.893000	0.750358	15	0.7128	4.59	22.18	0.21	0.125300	0.512059	14	–7.23	1876	1767

a) Analysis was performed on a Finnigan MAT-262 thermal ionization mass spectrometer (TIMS) in the Laboratory for Radiogenic Isotope Geochemistry, Institute of Geology and Geophysics, Chinese Academy of Sciences, Beijing. $^{143}Nd/^{144}Nd$ ratios were normalised to $^{146}Nd/^{144}Nd=0.7219$ and $^{87}Sr/^{86}Sr$ ratios to $^{86}Sr/^{88}Sr=0.1194$. Repeated measurements of BCR-1 for the $^{143}Nd/^{144}Nd$ ratio and NBS987 for the $^{87}Sr/^{86}Sr$ ratio gave mean values of 0.512638±30 (2σ) and 0.710226±12 ($n = 8$). "—"not analysed.

** Shen W Z, Ling H F, Sun T, et al. Nd-Sr isotope study of Late Mesozoic granite-volcanic rocks in South China. Petrogenesis and Lithospheric Dynamics Evolvement of late Mesozoic Granites in Nanling Region, unpublished.

$\lambda_{Rb} = 1.42\times10^{-11}$/a; $\lambda_{Sm} = 6.54\times10^{-12}$/a; Sm-Nd isotope compositions of depleted mantle according to $^{143}Nd/^{144}Nd = 0.513151$; $^{147}Sm/^{144}Nd = 0.2136$.

since the Early-Middle Jurassic[14,54−57]. Cretaceous volcanic-intrusive rocks in western Guangdong and intermediate-acidic igneous rocks in the coastal area of Zhejiang and Fujian share similar geochemical characteristics, such as high-K calc-alkaline features and similarity in spider diagram and rare earth element patterns, which implies that they should be formed under similar tectonic settings. Several trace element discrimination diagrams were tested. The Cretaceous volcanic-intrusive rocks were plotted on the boundary of the "late collision-post collision granite" and "volcanic arc granite" area on the Rb/30-Hf-Ta*3 diagram (Fig. 10), and plotted in the "volcanic arc granites" areas approaching to the joint point of "volcanic arc granite", "syn-collision granite", and "within plate granite" on the Rb–(Y+Nb) diagram (Fig. 11), which is thought to be an indicator of post collision tectonic setting by Pearce[58] and Förster[59]. Therefore, compared with Late Mesozoic igneous rocks in the coastal areas of Zhejiang and Fujian, the Cretaceous volcanic-intrusive magmatism in western Guangdong is likely to have a similar tectonic setting. However, the protoliths may be different as western Guangdong is located inland and far from the subduction zone, and further study may be required to make it clearer.

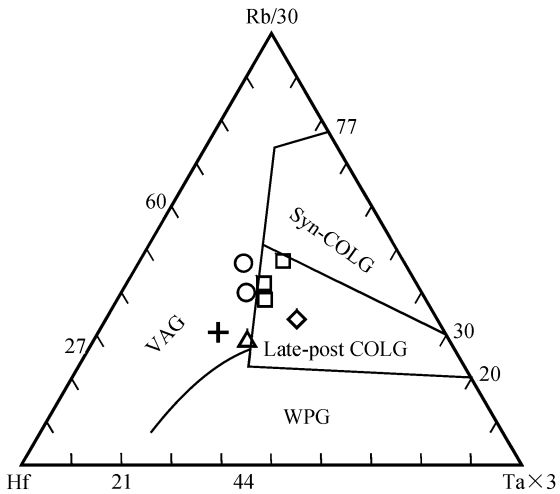

Fig. 10. Rb/30-Hf-Ta*3 discrimination diagram for Cretaceous volcanic-intrusive rocks. Symbols as in Fig. 3. VAG = volcanic arc granite; WPG = within plate granite; late-post COLG = late-post collision granite; Syn-COLG = syn-collision granite.

Consequently, the occurrence of Cretaceous volcanic-intrusive rocks offers a clue to the Pacific tectonic regime's influence on inland areas. About 100 Ma ago, there was an important lithospheric extension event in Southeast China with the Nanling Mountains included[41,60]. The partial melting of Proterozoic crust basement produced Cretaceous magma which ascended along the Lianxian-Yunan fault, and formed the Cretaceous rhyodacite and simultaneously the Deqing, Xinghua, and Tiaocun granitic bodies.

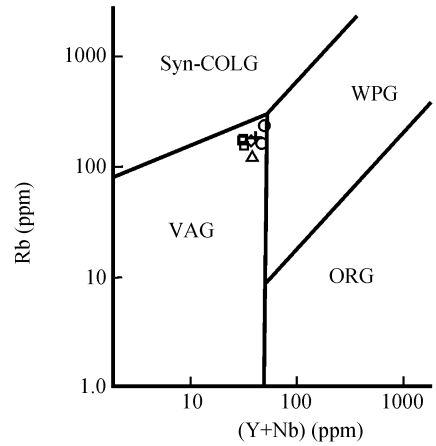

Fig. 11. Rb-(Y+Nb) discrimination diagram for Cretaceous volcanic-intrusive rocks. Symbols as in Fig. 3. VAG = volcanic arc granite; ORG = ocean ridge granite; WPG = within plate granite; Syn-COLG = syn-collision granite.

In the light of the distribution of Late Mesozoic intermediate-acidic volcanic rocks in Southeast China, Zhou and Li[48] proposed a "volcanic line" which is almost coincident with the Ganjiang fault and 450 km away from the coastline of Zhejiang and Fujian provinces. To the east of the "volcanic line", intermediate-acidic volcanic rocks are widespread, while to the west they have little distribution. However, the location of the southward continuation of the volcanic line was uncertain (in Zhou and Li's paper[48], it was marked with dashed line). The occurrence of rhyodactie in Jiancheng and Zhougongding basins in western Guangdong enables us now to draw the "volcanic line" southwestward to the Lianxian-Yunan fault (Fig. 1). The latter, together with the Ganjiang fault, formed a giant fault belt in East China.

6 Conclusion

(1) LA-ICP-MS zircon U-Pb isotope dating shows that the age of Ma'anshan rhyodacite is 100±1 Ma, and those of Deqing and Tiaocun bodies are 99±2 Ma, 104±3 Ma respectively. Zircon U-Pb isotope dating

together with biotite-plagioclase-whole rock Rb-Sr isochron dating shows that the Xinghua body formed at ca. 100 Ma. So Cretaceous (ca. 100 Ma) volcanic-intrusive magmatism exists in western Guangdong. The main bodies of the Shidong and Guangping complexes, with ages of 461±35 Ma, 444±6 Ma respectively, are the products of Caledonian magmatisms.

(2) Cretaceous volcanic-intrusive rocks as well as the Caledonian intrusive rocks are all characterized by high-K calc-alkali features, enrichment in Rb, Th, Ce, Zr, Hf, Sm, depletion in Ba, Nb, Ta, P, Ti, and weak REE tetrad effects. But there are some differences in the negative Eu anomalies with Caledonian intrusive rocks showing the most distinct one, and Cretaceous volcanic rocks having the least distinct. Studies of Sr-Nd isotopes show that the Cretaceous rhyodacite, granitoids, and the Caledonian biotite granite all have high $(^{87}Sr/^{86}Sr)_i$ values (0.7105－0.7518), low $\varepsilon_{Nd}(t)$ values (−7.23 to −11.39), and two-stage Nd modal ages (T_{2DM}) ranging from 1.6 to 2.0 Ga, which indicate that they may all derive from the Proterozoic crust basement by partial melting processes.

(3) The petrochemical features of Cretaceous volcanic-intrusive magmatism in western Guangdong are similar to those of the Late Mesozoic volcanic-intrusive magmatisms in the coastal area of Zhejiang and Fujian, and were formed in extensional tectonic settings. The occurrences of Cretaceous intermediate-acidic volcanic rocks in western Guangdong now enable us to extend the "volcanic line" southwestward.

Acknowledgements We appreciate Dr Chu Z. Y. who offered great help on the Sr-Nd isotope analysis. This paper has benefited from the helpful and constructive comments of the two anonymous reviewers. We would like also to thank Dr O'Hara M. J. and Dr O'Hara Susan for the helpful discussion. This work was supported by the National Natural Science Foundation of China (Grant Nos. 40221301, 40125007 and 40132010).

References

1. Shu L S, Deng P, Wang B, et al. Lithology, kinematics and geochronology related to Late Mesozoic basin-mountain evolution in the Nanxiong-Zhuguang area, South China. Sci China Ser D-Earth Sci, 2004, 47(8): 673－688
2. Shen W Z, Ling H F, Li W X, et al. Study on the Nd-Sr isotopic compositions of granitoids in SE China. Geol J Chin Univ (in Chinese with English abstract), 1999, 5(1): 22－32
3. Sun T, Zhou X M, Chen P R, et al. Strongly peraluminous granites of Mesozoic in Eastern Nanling Range, southern China: Petrogenesis and implications for tectonics. Sci China Ser D-Earth Sci, 2005, 48(2): 165－174
4. Zhang M, Chen P R, Zhang W L, et al. Geochemical characteristics and petrogenesis of Dadongshan granite pluton in mid Nanling Range. Geochimica (in Chinese with English abstract), 2003, 32(6): 529－539
5. Wang Y J, Fan W M, Guo F, et al. Geochemistry of Mesozoic granodioritic intrusions in Southeastern Hunan Province. Acta Petrol Sin (in Chinese with English abstract), 2001, 17(1): 169－175
6. Wang Y J, Fan W M, Guo F, et al. U-Pb dating of Mesozoic granodioritic intrusions in Southeastern Hunan Province and its petrogenetic implications. Sci China Ser D-Earth Sci, 2002, 45(3): 280－288
7. Li X H, Chen Z G, Liu D Y, et al. Jurassic gabbro-granite-syenite suites from southern Jiangxi Province, SE China: age, origin, and tectonic significance. Int Geol Rev, 2003, 45: 898－921
8. Wang Y J, Fan W M, Guo F. Geochemistry of early Mesozoic potassium-rich diorites-granodiorites in southeastern Hunan Province, South China: Petrology and tectonic implications. Geochem J, 2003, 37: 427－448
9. Liu C S, Chen X M, Wang R C, et al. Origin of Nankunshan aluminous A-type granite, Longkou County, Guangdong Province. Acta Petrol Mineral (in Chinese with English abstract), 2003, 22(1): 1－10
10. Liu C S, Chen X M, Wang R C, et al. Characteristic and origin of the shilling sodalite syenite, Conghua City, Guangdong Province. Geol Rev (in Chinese with English abstract), 2003, 49(1): 28－39
11. Liu C S, Chen X M, Wang R C, et al. Mineralogic characteristics and genesis for Shiling sodalite syenite, Nanling area, South China. Acta Mineral Sin (in Chinese with English abstract), 2002, 22(3): 261－269
12. National Compiling Group on Geological Isotope Age Data. National Isotope Compilation on Geological Age Data (3rd version) (in Chinese). Beijing: Geological Publishing House, 1983. 338－339
13. Yu J S, Gui X T, Li P Z, et al. Isotopic, minor elements studies of granitoids in Yangchun basin Guangdong Province. Guangdong Geology (in Chinese), 1998, 13(3): 1－9
14. Li X H, Zhou H W, Liu Y, et al. Mesozoic shoshonitic intrusives in the Yangchun Basin, western Guangdong, and their tectonic significance: I. Petrology and isotope geochronology. Geochimica (in Chinese with English abstract), 2000, 29(6): 513－520
15. Bureau of Geology and Mineral Resources of Guangdong Province. Instructions for Geological Map (1∶200000) of China: Luoding session (in Chinese), 1964, 111

16. Bureau of Geology and Mineral Resources of Guangxi Province. Instructions for Geology and Mineral Resources Map (1∶200000) of China: Wuzhou session (in Chinese), 1965, 38－54
17. Wu G Y, Zhang Y Z. The geochronology of Guangning granitic complex. Guangdong Geology (in Chinese), 1986, 1(1): 1－22
18. Bureau of Geology and Mineral Resources of Guangdong Province. Instructions for Geological Map (1: 200000) of China: Gaoyao session (in Chinese), 1964
19. Bureau of Geology and Mineral Resources of Guangdong Province. Instructions for Geological Map (1∶200000) of China: Huaiji session (in Chinese), 1964, 48
20. Geology and Mineral Resources Bureau of Guangxi Province. Regional Geology of Guangxi Province (in Chinese). Beijing: Geological Publishing House, 1985. 356
21. Geology and Mineral Resources Bureau of Guangdong Province. Regional Geology of Guangdong Province (in Chinese). Beijing: Geological Publishing House, 1988. 494
22. Wang L K, Sha L K, Xu W X, et al. The Theory of Granite Formation and Series. Guangzhou (in Chinese), Guangdong Science & Technology Press, 2003. 113
23. Middlemost E A K. Naming materials in the magma/igneous rock system. Earth Sci Rev, 1994, 37: 215－224
24. Irvine T N, Baragar W R A. A guide to the chemical classification of the common volcanic rocks. Can J Earth Sci, 1971, 8: 523－548
25. Peccerillo A, Taylor S R, Geochemistry of Eocene calc-alkaline volcanic rocks of the Kastamonu area, northern Turkey. Contrib Mineral Petrol, 1976, 58: 63－81
26. Li W X, Zhou X M. Geochemical constrains on the petrogenesis of Late Mesozoic igneous rocks in coastal area of Zhejiang and Fujian Province. Prog Nat Sci, 2000, 10(7): 630－641
27. Xie X, Xu X S, Xing G F, et al. Geochemistry and genesis of early Cretaceous volcanic rock assemblages in eastern Zhejiang. Acta Petrol Sin (in Chinese with English abstract), 2003, 19(3): 385－398
28. Pearce J A. Role of the sub-continental lithosphere in magma genesis at active continental margins. In: Hawkesworth C J, Norry M J, eds. Continental Basalts and Mantle Xenoliths Nantwich: Shiva, 1983, 230－249
29. Taylor S R, McLennan S M. The Continental Crust: Its Composition and Evolution. Oxford: Blackwell, 1985
30. Irber W. The lanthanide tetrad effect and its correlation with K/Rb, Eu/Eu*, Sr/Eu, Y/Ho, and Zr/Hf of evolving peraluminous granite suites. Geochim Cosmochim Acta, 1999, 63: 489－508
31. Zhao Z H, Xiong X L, Han X D. A discussion on the genetic mechanism of REE tetrad effect of granites——A case study from Qianlishan and Baerze granites in China. Sci China Ser D-Earch Sci, 1999, 29(4): 331－338
32. Poller U, Liebetrau V, Todt W. U-Pb single-zircon dating under cathodoluminescence control (CLC-method): application to polymetamorphic orthogneisses. Chem Geol, 1997, 139: 287－297
33. Xu X S, Deng P, O'Reilly S Y, et al. Single zircon LAM-ICPMS U-Pb dating of Guidong complex (SE China) and its petrogenetic significance. Chin Sci Bull, 2003, 48(17): 1892－1899
34. Ludwig K R. Isoplot——a geochronological toolkit for Microsoft Excel: Berkeley Geochronology Center Special Publication, 2000, No 1a
35. Griffin W L, Belousova E A, Shee S R, et al. Crustal evolution in the northern Yilarn Craton: U-Pb and Hf-isotope evidence from detrital zircons. Precambrian Research, 2004, 131: 231－282
36. Shen W Z, Zhu J C, Liu C S, et al. Sm-Nd isotopic study of basement metamorphic rocks in South China and its constraint on material sources of granitoids. Acta Petrol Sin (in Chinese with English abstract), 1993, 9(2): 115－124
37. Jahn B M, Condie K C. Evolution of the Kaapvaal Craton as viewed from geochemical and Sm-Nd isotopic analyses of intracratonic pelites. Geochim Cosmochim Acta, 1995, 59: 2239－2258
38. Chen J F, Jahn B M. Crustal evolution of southeastern China: Nd and Sr isotopic evidence. Tectonophysics, 1998, 284: 101－133
39. Xu X S, O'Reilly S Y, Griffin W L, et al. Relict Proterozoic basement in the Nanling Mountain (SE China) and its tectonothermal overprinting. Tectonics, 2005, 24, doi: 10.1029
40. Gilder S A, Keller G R, Luo M, et al. Timing and spatial distribution of rifting in China. Tectonophysics, 1991, 197: 225－243
41. Gilder S A, Gill J, Coe R S, et al. Isotopic and paleomagnetic constrains on the Mesozoic tectonic evolution of South China. J Geophys Res, 1996, 101: 16137－16154
42. Li X H, McCulloch M T. Geochemical characteristics of Cretaceous mafic dikes from northern Guangdong, SE China: Age, origin and tectonic significance. In: Flower M F J, Chung S L, Lo C H, et al. eds. Mantle Dynamics and Plate Interaction in East Asia Geodynamics 27. American Geophysical Union, Washington D C, 1998. 405－419
43. Li X H. Cretaceous magmatism and lithospheric extension in Southeast China. J Asian Earth Sci, 2000, 18: 293－305
44. Xie X, Xu X S, Zou H B, et al. Early J2 basalts in SE China: Incipience of large-scale late Mesozoic magmatism. Sci China Ser D-Earth Sci (in Chinese), 2005, 35(7): 587－605
45. Wang Y J, Fan W M, Peng T P, et al. Element and Sr-Nd systematics of early Mesozoic volcanic sequence in southern Jiangxi Province, South China: petrogenesis and tectonic implications. Int J Earth Sci, 2005, 1: 53－65
46. Engebretson D C, Cox A, Gordon R G. Relative motions between oceanic and continental plates in the Pacific basin. Geol Soc Am Spec, 1985, Paper: 1－59
47. Maruyama S, Seno T. Orogeny and relative plate motions: example of Japanese islands. Tectonophysics, 1986, 127: 305－329
48. Zhou X M, Li W X. Origin of Late Mesozoic igneous rocks of Southeastern China: implications for lithosphere subduction and underplating of mafic magma. Tectonophysics, 2000, 326: 269－287
49. Xu X S, Xie X. Late Mesozoic-Cenozoic basaltic rocks and

crust-mantle interaction, SE China. Geol J China Univ (in Chinese), 2005, 11(3): 318－334

50. Martin H, Bonin B, Capdevila R, et al. The Kuiqi peralkaline granitic complex (SE China): Petrology and geochemistry. J Petrol, 1994, 35: 983－1015
51. Zhou X R, Wu K L, Yan B Q, et al. I-A Type Granite in Zhangzhou (in Chinese). Beijing: Science Press, 1994. 1－148
52. Chen J F, Zhou T X, Li X M, et al. Sr-Nd isotope composition and its tectonic significance of Mesozoic igneous rocks in Southeast China. In: Li J L, ed. Study on Structure and Evolution for Oceanic and Continental Lithosphere of Southeast China (in Chinese). Beijing: Science and Technology Press of China, 1992. 119－130
53. Wang Y X, Zhao Z H, Bao Z W, et al. Geochemistry of granitoids from Zhejiang province and crustal evolution-I. Phanerozoic granitoids. Geochimica (in Chinese with English abstract), 1997, 26(5): 1－15
54. Li X H, Zhou H W, Liu Y, et al. Mesozoic shoshonitic intrusives in the Yangchun Basin, western Guangdong, and their tectonic significance: Ⅱ. Trace elements and Sr-Nd isotopes. Geochimica (in Chinese with English abstract), 2001, 30(1): 57－65
55. Li X H, Zhou H W, Liu W, et al. Shoshonitic intrusive suite in SE Guangxi: Petrology and geochemistry. Chin Sci Bull, 2000, 45(7): 653－658
56. Harris H B W, Pearce J A, Tindle A G. Geochemical characteristics of collision-zone magmatism. In: Coward M P, Reis A G, eds. Collision Tectonics, Spec Publ Geol Soc Lond, 1986, 19: 67－81
57. Pearce J A, Harris N B W, Tindle A G. Trace element discrimination diagram for the tectonic interpretation of granitic rocks. J Petrol, 1984, 25: 956－983
58. Pearce J A. Sources and settings of granitic rocks. Episodes, 1996, 19: 120－125
59. Förster H J, Tischendorf G, Trumbull R B. An evaluation of the Rb vs. (Y+Nb) discrimination diagram to infer tectonic setting of silicic igneous rocks. Lithos, 1997, 40: 261－293
60. Lo C H, Lee C Y. ^{40}Ar-^{39}Ar method of the K-Ar age determination on geological samples using Tsing Hua Open Pool (THOR) reactor. J Geol Soc of Chin, 1994, 37(2): 1－22